L-Arginyl-3,4-Spermidine is neuroprotective in several *in vitro* models of neurodegeneration and *in vivo* ischaemia without suppressing synaptic transmission

*,[1]Barclay Morrison III, [1]Ashley K. Pringle, [1]Terence McManus, [2]John Ellard, [2]Mark Bradley, [1]Francesco Signorelli, [1]Fausto Iannotti & [1]Lars E. Sundstrom

[1]Division of Clinical Neurosciences, School of Medicine, Bassett Crescent East, University of Southampton, Southampton, SO16 7PX and [2]Combinatorial Centre of Excellence, Highfield, University of Southampton, Southampton, SO17 1BJ

1 Stroke is the third most common cause of death in the world, and there is a clear need to develop new therapeutics for the stroke victim. To address this need, we generated a combinatorial library of polyamine compounds based on sFTX-3.3 toxin from which L-Arginyl-3,4-Spermidine (L-Arg-3,4) emerged as a lead neuroprotective compound. In the present study, we have extended earlier results to examine the compound's neuroprotective actions in greater detail.

2 In an *in vitro* ischaemia model, L-Arg-3,4 significantly reduced CA1 cell death when administered prior to induction of 60 min of ischaemia as well as when administered immediately after ischaemia. Surprisingly, L-Arg-3,4 continued to prevent cell death significantly when administration was delayed for as long as 60 min after ischaemia.

3 L-Arg-3,4 significantly reduced cell death in excitotoxicity models mediated by glutamate, NMDA, AMPA, or kainate. Unlike glutamate receptor antagonists, 300 μM L-Arg-3,4 did not suppress synaptic transmission as measured by evoked responses in acute hippocampal slices.

4 L-Arg-3,4 provided significant protection, *in vitro*, in a superoxide mediated injury model and prevented an increase of superoxide production after AMPA or NMDA stimulation. It also decreased nitric oxide production after *in vitro* ischaemia and NMDA stimulation, but did so without inhibiting nitric oxide synthase directly.

5 Furthermore, L-Arg-3,4 was significantly neuroprotective in an *in vivo* model of global forebrain ischaemia, without any apparent neurological side-effects.

6 Taken together, these results demonstrate that L-Arg-3,4 is protective in several models of neurodegeneration and may have potential as a new therapeutic compound for the treatment of stroke, trauma, and other neurodegenerative diseases.
British Journal of Pharmacology (2002) **137,** 1255–1268. doi:10.1038/sj.bjp.0704986

Introduction

Stroke is the third most common cause of death in the world after coronary heart disease and cancer with an incidence of approximately 400 per 100,000 population (Murray & Lopez, 1997). Approximately 20% of stroke patients do not survive longer than 1 month, and a third of those that are still alive after 6 months are dependent on others (Warlow, 1998). Currently, the only approved treatments are thrombolitic agents such as tissue plasminogen activator which must be initiated within 3 h of onset and are indicated for a particularly small percentage of patients (1–2%) (Fisher & Schaebitz, 2000). Clearly there is a need to develop new therapeutic strategies for the stroke victim.

Periods of cerebral ischaemia activate a complex cascade which results in neuronal cell death and dysfunction responsible for the debilitating effects of various CNS disorders including stroke and traumatic brain injury as well as other neurodegenerative conditions. The failure of aerobic glycolysis and subsequent depletion of cellular energy stores are proximal events in the ischaemic sequelae which lead to a disruption of ion homeostasis causing neurons to depolarize (Kristian & Siesjo, 1998). This depolarization initiates the opening of voltage sensitive calcium channels (VSCC) and the release of neurotransmitters which, in turn, activate receptor gated ion channels allowing Na$^+$ and Ca^{2+} to enter the cell. Several second messenger systems are activated by elevated intracellular Ca^{2+} that can generate reactive oxygen species (ROS) which damage lipid membranes and other

*Author for correspondence; E-mail: B.Morrison@soton.ac.uk

cellular components. Under conditions of Ca^{2+} overload, mitochondria can become a significant source of free-radicals, overwhelm endogenous scavenging systems, and damage cellular components (Piantadosi & Zhang, 1996). Any one of these pathophysiological steps in this cascade could be a potential therapeutic target for reducing ischaemic cell death.

The venom of the funnel web spider *Agelenopsis aperta* contains a mixture of toxins including a fraction termed FTX which blocks P-type VSCC in rat Purkinje neurons and cortical synaptosomes (Llinas *et al.*, 1989; Cherksey *et al.*, 1991). The active component of crude FTX, called FTX-3,3, has been isolated and identified, and an analogue, termed sFTX-3.3 which differs from FTX-3.3 in a single carbonyl group, has been synthesized (Figure 1). The electrophysiological properties of both these compounds have been studied in some detail demonstrating that both preferentially block P-type VSCC with an IC_{50} near 240 nM but also block N- and neuronal L-type VSCC at concentrations above 1 μM (Cherksey *et al.*, 1991; Dupere *et al.*, 1996). Because of the potential involvement of VSCC in cellular Ca^{2+} loading during ischaemic depolarization, these toxins, in modified form, could be useful neuroprotective agents. Therefore, a program was initiated to determine if such polyamine compounds could be synthesized that were non-toxic as well as neuroprotective. A library of compounds, loosely based on the structure of sFTX-3.3, was generated *via* solid support combinatorial chemistry from which, L-Arginyl-3,4-Spermidine (L-Arg-3,4), emerged as a lead compound from an *in vitro* screen against hypoxia in organotypic brain slice cultures. This *in vitro* model represents an attractive alternative to *in vivo* models by providing greater accessibility to the tissue and control of the extracellular milieu while maintaining hallmark features

seen *in vivo*. Such hallmark features include the selective vulnerability of specific pyramidal cell layers to different injury paradigms i.e. the CA1 pyramidal cell layer is more vulnerable to hypoxic and NMDA receptor-mediated excitotoxic injuries, whereas CA3 is more vulnerable to kainite receptor-mediated toxicity. In addition, the subsequent neuronal cell death is delayed and demonstrates a similar temporal profile to that seen *in vivo* (Pringle *et al.*, 1996; 1997).

In this study, we extend earlier findings and show that L-Arg-3,4 is protective in several *in vitro* models of neuronal cell death including a severe ischaemia paradigm as well as excitatory amino acid (EAA) and free-radical mediated cell death. Furthermore, in preliminary *in vivo* experiments, this compound reduced CA1 pyramidal cell loss due to transient forebrain ischaemia after four vessel occlusion in the rat. These results suggest that L-Arg-3,4 is a novel, neuroprotective compound in multiple models of cell death and that it warrants more detailed testing *in vivo*.

Methods

Drugs

Kainate, NMDA, glutamate, AMPA, 6,7-Dinitroquinoxaline-2,3(1H,4H)-dione (DNQX), and N-nitro-L-arginine methyl ester (L-NAME) were purchased from Sigma (U.K.). DNQX was stored at room temperature in dimethylsulphoxide (DMSO) at 40 mM. All other drugs were made up as aqueous solutions.

Chemicals and reagents

Propidium iodide (PI) and hydroethidine (HEt) were purchased form Molecular Probes (Eugene, OR, U.S.A.). 4,5-Diaminofluorescein diacetate (DAF-2) was purchased from Calbiochem (U.K.). DMSO, glucose, glutamine, NaCl, EDTA, dithiothreitol (DTT), HEPES, glycerophosphate, NaF, $NaVO_3$, Triton X-100, and arginine were purchased from Sigma. Millicell CM culture inserts were purchased from Millipore (U.K.). The 1N-Dde-8N-Mmt-spermidine-4-yl)-carbonyl Wang polystyrene resin was purchased from Novabiochem (Switzerland), and the Fmoc-Arg(Boc)$_2$-OH from Bayer (U.K.). All other chemicals and reagents were obtained from commercial sources except for L-Arg-3,4 which was synthesized as indicated below.

L-Arg-3,4 trifluoroacetic acid salt synthesis

(1N-1-(4,4-dimethyl-2,6-dioxocyclohexylidene)ethyl-8N-mono-methyltrityl-spermidine-4-yl)-carbonyl Wang polystyrene resin (0.279 g, loading 0.42 mmol g^{-1}, 0.12 mmol) was swollen in *N,N*-dimethylformamide (DMF). The solvent was then drained and 2% hydrazine in DMF (4 ml) was added. The resulting mixture was spun for 5 min. The solution was drained and the hydrazinolysis repeated twice more. The resin was then washed with DMF ($\times$3), DCM ($\times$3), and diethyl ether ($\times$3). A qualitative ninhydrin test was positive.

The resin was then swollen in DMF and the solvent drained. A solution of 9-fluorenylmethoxycarbonyl-Arginine-
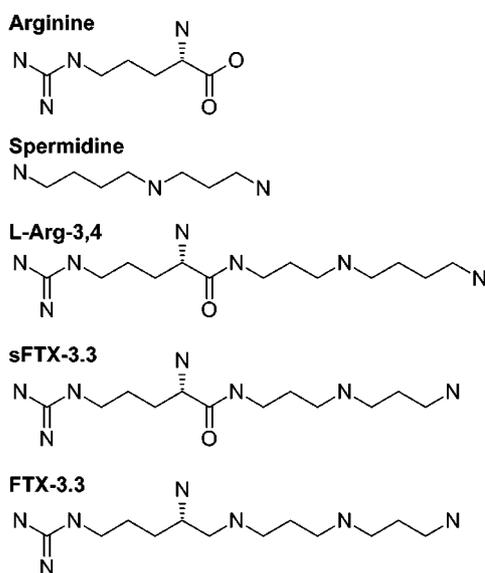

Figure 1 Structures of compounds related to L-Arg-3,4 which is a heterodimer of arginine and spermidine. The structure of L-Arg-3,4 is similar to a toxin from the venom of *A. aperta* termed FTX-3.3. A synthetic analogue to FTX-3.3, termed sFTX-3.3, has been chemically synthesized and contains an additional carboxyl group which is not present in the naturally occurring toxin.

(*tert*-butyloxycarbonyl)$_2$-OH (0.142 g, 0.24 mmol, 0.24 M) and *N*-hydroxybenzotriazole hydrate (0.037 g, 0.24 mmol, 0.24 M) in dichloromethane (DCM) (0.6 ml) and DMF (0.4 ml) were stirred at room temperature for 10 min, diisopropylcarbodiimide (38 μl, 0.24 mmol) was added and the resulting solution stirred for a further 10 min. The reaction mixture was then added to the damp resin and spun for 2.5 h. The solution was drained and the resin washed with DMF ($\times$3), DCM ($\times$3) and diethyl ether ($\times$3). A qualitative ninhydrin test was negative.

The resin was swollen in DMF and the solvent drained. A 20% piperidine solution in DMF (4 ml) was added and the reaction mixture was spun for 10 min. The solution was drained and the piperidine treatment repeated. The resin was washed with DMF ($\times$3), DCM ($\times$3) and diethyl ether ($\times$3). A quantitative ninhydrin test was positive.

To the dry resin was added a solution of 97.5% trifluoroacetic acid (TFA) and 2.5% triisopropylsilane (4 ml), and the reaction mixture allowed to stand for 3 h. The solvent was then drained and the resin washed with TFA (2×1 ml). The combined acid phases were evaporated *in vacuo*. The residue was dissolved in TFA (0.4 ml) and precipitated in ice-cold diethyl ether. The mixture was centrifuged and the solvent removed by decanting. The pellet was washed with diethyl ether, the mixture centrifuged, and the solvent again decanted. The residue was then dried *in vacuo* overnight. The residue was dissolved in TFA (0.4 ml) and the diethyl ether precipitation repeated. The sample was then dissolved in water and acetonitrile and lyophilized. This was repeated once more to afford L-Arg-3,4 as a sticky orange-brown solid (0.061 g, 20% L-Arg-3,4 by mass). The polyamine was quantified by ^{1}H nuclear magnetic resonance spectroscopy with phenol as an internal standard.

Organotypic cultures

Organotypic hippocampal slice cultures were prepared according to established methods (Pringle *et al.*, 1997), and all animal procedures were approved by the Home Office. In brief, Wistar rat pups (8 – 11 days old) were decapitated and the hippocampus rapidly dissected into ice-cold Gey's balanced salt solution (Gibco Life Technologies, Paisley, U.K.) supplemented with 4.5 mg ml^{-1} glucose. Slices were separated and plated onto Millicell CM culture inserts (four per well) and maintained at 37°C and 5% CO$_2$ for 14 days. Maintenance medium consisted of 25% heat-inactivated horse serum, 25% Hank's balanced salt solution (HBSS) and 50% minimum essential medium with added Earle's salts (MEM, ICN Biomedicals, Basingstoke, U.K.) supplemented with 1 mM glutamine and 4.5 mg ml^{-1} glucose. Medium was changed every 3 – 4 days.

Ischaemic injury

Experimental ischaemia or oxygen glucose deprivation was performed as described previously (Pringle *et al.*, 1996). Briefly, cultures were transferred to serum free media (SFM, 75% MEM, 25% HBSS supplemented with 1 mM glutamine and 4.5 mg ml^{-1} glucose) containing 5 μg ml^{-1} of the fluorescent exclusion dye propidium iodide (PI). Cultures were allowed to equilibrate in SFM for 30 min prior to imaging, with or without L-Arg-3,4. PI fluorescence was

detected using a Leica inverted microscope as described below. Any cultures in which PI fluorescence was detected at this stage were excluded from further study. Ischaemia was induced by transferring cultures to glucose free media (MEM with Earl's salts without glucose and supplemented with 1 mM glutamine) saturated with 95% N$_2$ and 5% CO$_2$. Culture plates (without lids) were then sealed into an airtight chamber (Billups-Rothenberg, Del Mar, CA, U.S.A.) gassed with 95% N$_2$ and 5% CO$_2$ at 10 L min^{-1} for 10 min before being sealed and placed at 37°C for 50 min. At the end of the ischaemia, cultures were returned to normoxic SFM + PI, with or without compound at the indicated concentrations, and placed back in the incubator for 24 h.

Excitotoxic injury

Excitotoxic injury was performed as previously described (Pringle *et al.*, 1997) with L-Arg-3,4 present pre-, during, and post-injury in treated cultures. Cultures were transferred to SFM + PI with or without 300 μM L-Arg-3,4 and allowed to equilibrate for 30 min prior to imaging. Any cultures exhibiting PI fluorescence were excluded. The medium was then exchanged for SFM + PI plus a glutamate receptor agonist (either 10 mM glutamate, 10 μM NMDA, 10 μM AMPA, or 10 μM kainate) for 3 h. After exposure, the media was again exchanged for SFM + PI containing 300 μM L-Arg-3,4. Cultures were then returned to the incubator until they were assessed for cell death in the indicated region of the pyramidal cell layer 24 h post exposure.

Free-radical injury

Free-radical mediated injury was performed as described previously with L-Arg-3,4 present pre-, during, and post-injury in treated cultures (Wilde *et al.*, 1997). Briefly, cultures were transferred to SFM + PI with or without 300 μM L-Arg-3,4 and allowed to equilibrate for 30 min prior to imaging. Any cultures in which PI fluorescence was detected at this stage were excluded from further study. Duroquinone was dissolved in DMSO at a stock concentration of 100 mM which was then diluted 1:1000 in SFM for a final working concentration of 100 μM (final DMSO concentration of 0.1%). Free-radical injury was initiated by transferring cultures to SFM supplemented with 100 μM duroquinone for 3 h. At the end of the exposure, cultures were returned to SFM + PI, with or without compound, and placed in the incubator for 24 h.

Assessment of cell death

Neuronal damage was assessed as described previously (Pringle *et al.*, 1996; 1997). Light transmission images were captured prior to the induction of injury, and PI fluorescence images recorded at the end of the 24 h post-injury recovery period. Injury paradigms produced stereotypical patterns of injury shown in Figure 2. All images were captured on an inverted Leica DM-IRBE epiflourescence microscope (Milton Keynes, U.K.) fitted with a 100 W Hg lamp and standard rhodamine optics (excitation 510 – 560 nm; dichroic mirror 620 nm; emission > 590 nm). Images were acquired with a 5 $\times$ NA 0.12 lens and a cooled Hamamatsu digital camera and digitized at 12 bit resolution for analysis in OpenLab 2.1
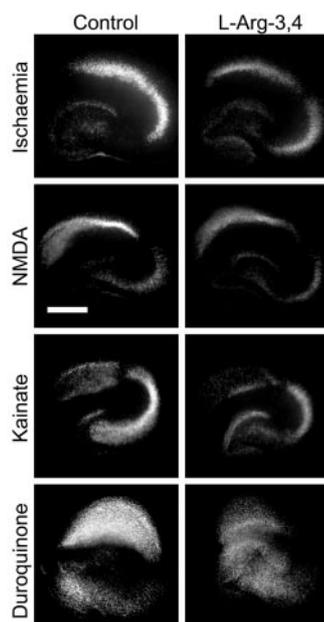
Figure 2 Propidium iodide fluorescence micrographs of treated and untreated organotypic hippocampal cultures subjected to different injury paradigms. Cultures were prepared and injured as indicated in the Methods section. Organotypic slice cultures are ideal *in vitro* preparations to study neurodegeneration because the *in vivo* regional susceptibility of neuronal populations to different insults is maintained in culture. The ischaemic injury utilized in these studies is a severe injury and causes damage to both CA1 and CA3 cell layers. The damage to the CA1 cell layer was reduced by 300 μM L-Arg-3,4 as demonstrated in the micrograph of the treated culture. NMDA excitotoxicity caused PI uptake predominately in the CA1 pyramidal cell layer which was reduced by L-Arg-3,4. Kainate excitotoxicity resulted in PI uptake which was predominate in the CA3 cell layer and was reduced by L-Arg-3,4. Free-radical injury mediated by duroquinone produced a visibly different pattern of PI uptake which was predominant in the CA1 cell layer and was reduced by L-Arg-3,4. The protective actions of 300 μM L-Arg-3,4 were studied only in CA1 for all injury paradigms except for kainate excitotoxicity which was studied in CA3. All images were taken 24 h post-injury. Scale bar is 1 mm.

Figure 3 The steps to calculate CA1 damage are presented, and a similar procedure was used to calculate CA3 damage. Cell damage was calculated as the percentage of area of a particular pyramidal cell layer exhibiting PI fluorescence above a set threshold level. The CA1 pyramidal cell layer was outlined in a transmission image of a culture acquired before induction of injury, and the area calculated. A fluorescence image of the same culture was acquired 24 h post-injury indicating cell damage with PI staining. A threshold function was then applied to the grey scale fluorescence image transforming it into a binary image. The binary image was combined with the template outlining the CA1 with a binary and operation allowing for the calculation of the area of CA1 demonstrating a suprathreshold level of PI fluorescence. Damage was calculated as this area of PI fluorescence normalized to the total area of CA1.

(Improvision, Coventry, U.K.) running on a Macintosh G4/400. The area of the CA1 or CA3 cell layer was determined from the transmission image (see Figure 3 for a typical CA1 measurement), and the area of PI fluorescence in that cell layers was measured using the density slice function within OpenLab. Neuronal damage was expressed as a percentage of the area in which PI fluorescence was detected above threshold within a cell layer divided by the total area of that cell layer. Protection was calculated as the difference between the damage for a given well and the average damage in untreated controls divided by the average damage in untreated controls. Groups were compared against corresponding control groups using the two-tailed Student's *t*-test with significance indicated as * for $P < 0.05$, and ** for $P < 0.01$. Data is presented as mean $\pm$ s.e.mean.

Electrophysiology

All animal procedures to produce acute hippocampal slices were approved by the Home Office. Male, 250 g, Sprague-Dawley 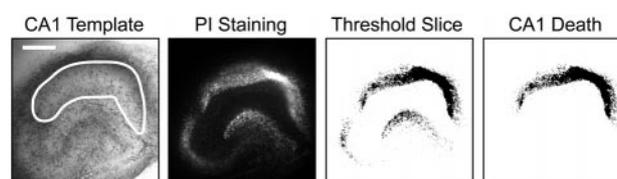rats were deeply anaesthetized with halothane and decapitated. The brain was quickly removed, and the hippocampi dissected out and then cut into 300 μm thick transverse slices on a vibratome (Leica, Milton Keynes, U.K.) in cold cutting solution (in mM): sucrose 189, KCl 2.5, NaHCO$_3$ 26, NaH$_2$PO$_4$ 1.2, glucose 10, MgCl$_2$ 5, CaCl$_2$ 0.1, equilibrated with 5% CO$_2$, 95% O$_2$. Slices were transferred to aCSF (in mM): glucose 10, NaCl 125, KCl 5, NaHCO$_3$ 26, MgCl$_2$ 1, NaH$_2$PO$_4$ 1.25, CaCl$_2$ 2, sucrose 10, at room temperature, bubbled with 5% CO$_2$ and 95% O$_2$, for at least 1 h before use.

Slices were then transferred to a submerged perfusion chamber (2 ml volume) for the electrophysiological recordings and were perfused at 10 ml min^{-1} at 25°C with aCSF equilibrated with 5% CO$_2$ and 95% O$_2$, and allowed to equilibrated for 1 h before manipulations were started. Experimental compounds were applied by bath perfusion. L-Arg-3,4 was applied at 300 μM and DNQX was applied at 10 μM final concentration. DNQX was diluted from a 40 mM stock in DMSO (final DMSO of 0.025%). The Schaffer collaterals of CA3 were stimulated at voltages from 0 to 30 V with a constant voltage stimulator (Digitimer, Hertfordshire, U.K.) *via* a twisted pair stimulating electrode of polyimide coated stainless steel wire (Plastics One, Roanoke, VA, U.S.A.). Field potential responses were recorded with an Axopatch 200B amplifier (Axon Instruments, Foster City, CA, U.S.A.) in the fast current clamp mode *via* a 2 M KCl filled glass electrode (2 – 5 MΩ) in the CA1 pyramidal cell layer. Responses were filtered at 2 kHz, digitized at 20 kHz with a Digidata 1320A (Axon Instruments), and stored onto hard disk with Clampex 8.1 software (Axon Instruments) running on a Dell Pentium III PC. Data was analysed in Clampfit 8.1 (Axon Instruments).

Stimulus-response (S/R) curves were generated from stimuli from 0 to 30 V in 2 V increments. Bath perfusion of 300 μM L-Arg-3,4 in aCSF was applied for 10 min with a sub-maximal stimulus applied every minute to monitor synaptic transmission. A second S/R curve was generated before the perfusion was switched back to plain aCSF. A sub-maximal stimulus was applied every minute during the 15 min wash period after which a third S/R curve was generated. Perfusion of 10 μM DNQX was then started until

the response to the sub-maximal stimulus was completely eliminated which always occurred within 10 min. Increasing the stimulus to maximum (30 V) did not generate a response, and therefore, no S/R curves were generated in the presence of DNQX. In Clampfit, S/R curves were fit to a sigmoidal function of the form:

$$R(S) = \frac{R_{Max}}{1 + e^{m \cdot (V_{50} - S)}} \qquad (1)$$

where R is the magnitude of the evoked response, R_{max} is the maximum response, V_{50} is the voltage which produces a half maximal response, S is the stimulus voltage, and m is proportional to the slope of the linear region of the sigmoid. Data was compared by one way ANOVA.

Measurement of superoxide production

As reported previously, hydroethidine (HEt) has been utlized to fluorescently monitor the production of superoxide in primary neuronal cultures (Bindokas *et al*., 1996; Carriedo *et al*., 1998). A stock solution of HEt was made in N_2 sparged DMSO (10 mg ml^{-1}) which was then aliquoted and stored at -80°C. Aliquots were used only once before being discarded. Two separate experimental paradigms were employed to test the effect of L-Arg-3,4 on superoxide production in response to either AMPA or NMDA stimulation.

For the AMPA experiments, organotypic slice cultures were loaded with 1 μg ml^{-1} HEt in HEPES buffered salt solution (HSS) (in mM): glucose 10, NaCl 144, KCl 5, HEPES 10, MgCl$_2$ 1, CaCl$_2$ 2, pH 7.4, for 30 min in the dark. All subsequent solutions contained HEt to prevent a decrease in signal due to reporter depletion. Images were acquired once per minute for the duration of the experiment on the same system as described above for assessment of cell death. A 10 min record of baseline superoxide production was produced before the bathing solution was exchanged for HBSS + HEt containing 10 μM AMPA, again for 10 min. As shown previously, stimulation of glutamate receptors with AMPA lead to an increase in superoxide production (Bindokas *et al*., 1996; Carriedo *et al*., 1998). The bathing solution was then exchanged for HSS + HEt containing both 10 μM AMPA and 300 μM L-Arg-3,4 for 10 min to test the effect of L-Arg-3,4 on superoxide production. In separate control experiments, 300 μM L-Arg-3,4 in HSS was incubated with slices to determine if it affected baseline superoxide production in its own.

Acquired images from the AMPA experiments were then analysed with the OpenLab image analysis package. A region of interest was drawn around the CA1 pyramidal cell layer because this was the cell layer that produced the largest increase in fluorescence in response to AMPA activation. In each image, within the region of interest, the average pixel value was calculated in arbitrary units (AU) to produce a record of fluorescence intensity values over time. A linear regression was then performed on the data to calculate the rate of superoxide production as change in intensity over time (arbitrary units per min, AU min^{-1}) for each of the treatments. Data is presented as mean $\pm$ s.d.. Rates of superoxide production were then compared by ANOVA followed by *post-hoc* comparisons with Bonferroni corrections with significance indicated as * for $P < 0.05$, and ** for $P < 0.01$.

For the NMDA experiments, cultures were loaded with 15 μM HEt in SFM for 2 h in the dark before being washed in PIPES buffered salt solution (in mM): CaCl$_2$ 5, KCl 5, MgCl$_2$ 2, NaCl 120, PIPES 20, glucose 20, pH 7.4, for 10 min at 37°C. Treated cultures were pre-loaded with 300 μM L-Arg-3,4 20 min before the start and throughout the duration of experiments. Cultures were then secured in a heated well on the stage of a confocal laser scanning microscope (Biorad MRC 1024ES) equipped with a krypton/argon laser (excitation 488 nm, emission 605 nm) so that superoxide production in single pyramidal neurons could be measured. With a 60 $\times$ water immersion objective, images were acquired during a 10 min baseline and then at 10 min intervals during stimulation with 500 μM NMDA in PIPES buffered salt solution. As shown previously, stimulation with 500 μM NMDA resulted in an increase of superoxide production which was readily measured by an increase of HEt fluorescence (Bindokas *et al*., 1996; Carriedo *et al*., 1998).

Acquired images were analysed with ScionImage (Scion Corp, Frederick, MD, U.S.A.) as follows. Regions of interest were drawn around individual, well-defined neurons in the CA1 pyramidal cell layer, and average pixel intensities calculated in arbitrary units. Cellular values were then normalized to the average pixel intensity calculated for that cell during the baseline period and then corrected for basal HEt conversion by subtracting the average normalized intensity from unstimulated control cultures. Data was compared by ANOVA followed by *post-hoc* comparisons with Bonferroni corrections with * indicating $P < 0.05$, and ** indicating $P < 0.01$. Data is presented as mean $\pm$ s.e.mean.

Measurement of nitric oxide generation

As reported previously (Brown *et al*., 1999), DAF-2 has been utilized to monitor the production of nitric oxide (NO) in acute hippocampal slices. DAF-2 was supplied as a solution in DMSO (1 mg ml^{-1}) and stored as per the manufacturer's instructions at 4°C. Three different paradigms were employed to measure the effect of L-Arg-3,4 on the production of NO. In two sets of experiments, organotypic cultures were loaded with 20 μM DAF-2 in SFM for 2 h in the dark before being washed in PIPES buffered salt solution. Treated cultures were pre-loaded with 300 μM L-Arg-3,4 20 min before the start and throughout the duration of experiments. Cultures were then secured in a heated well on the stage of a confocal laser scanning microscope (Biorad MRC 1024ES) equipped with a krypton/argon laser (excitation 488 nm, emission 515 nm) so that NO production could be measured either in the entire CA1 pyramidal cell layer with a 5 $\times$ objective or in individual CA1 pyramidal cells with a 60 $\times$ objective. In the first set of experiments, images were acquired before the induction and then after 60 min of ischaemia with the 5 $\times$ objective. Post-ischaemia images were analysed with ScionImage by drawing regions of interest around the CA1 pyramidal cell layer and calculating average pixel intensity normalized to the average pixel intensity before ischaemia. Data was compared with Student's two-tailed *t*-test.

In a second set of experiments, images were acquired with the 60 $\times$ objective during a 10 min baseline and then at 10 min intervals during stimulation with 500 μM NMDA. As shown previously, stimulation with 500 μM NMDA resulted

in an increase of NO production which was readily measured by an increase in DAF-2 fluorescence (Dawson *et al.*, 1991; Yamauchi *et al.*, 1998; Carriedo *et al.*, 1998). These images were analysed with ScionImage to calculate average pixel intensities within a whole field of view which were then normalized to the average baseline intensity and then corrected for basal DAF-2 conversion by subtracting the average normalized intensity from unstimulated control cultures. Data was compared by ANOVA followed by post-hoc comparisons with Bonferroni corrections with * indicating $P < 0.05$, and ** indicating $P < 0.01$. Data is presented as mean $\pm$ s.e.mean.

In a third set of experiments to directly test the effect of L-Arg-3,4 on nitric oxide synthase (NOS), fresh cortex was dissected from 11 day old rat pups and homogenized on ice at a ratio of 150 mg cortex per 1 ml of homogenization buffer (0.1% Triton X-100 plus, (in mM): NaCl 25, EDTA 2, DTT 0.5, HEPES 20, glycerolphosphate 20, NaF 50, NaVO$_3$ 1) with protease inhibitors (Roche Diagnostics, East Sussex, U.K.). The homogenate was centrifuged (Hettich, Germany) at $13,000 \times g$ for 4 min, and the supernatant removed and kept on ice until used. Duplicate 300 μl samples consisting of 20 μl of tissue extract, 5 μM DAF-2, 6 μM arginine plus the indicated concentrations of L-Arg-3,4 or L-NAME brought to volume with HSS were mixed in 24-well plates (Corning Costar, Bucks, U.K.). The plates were then read on a Fluorstar fluorescence plate reader (SLT LabInstruments, Germany) with the excitation filter set to 485 nm and the emission filter set to 538 nm. Fluorescence readings were acquired once per minute for 10 min, and the rate of NO formation (arbitrary units per min, AU min^{-1}) was calculated by a least squares linear fit to the data. Blank samples consisting of the above components but with either tissue extract or DAF-2 omitted did not increase fluorescence intensity over time. Experiments were repeated a total of four times. Groups were compared against controls using the two-tailed Student's *t*-test with significance indicated as * for $P < 0.05$, and ** for $P < 0.01$. Data is presented as mean $\pm$ s.d..

Blood flow studies

All animal procedures were approved by the Home Office. Adult male Wistar rats (250 – 300 g) were initially anaesthetized with 4% halothane anaesthesia maintained with 1.5% halothane mixed in 7% N$_2$O in O$_2$. The femoral artery was cannulated for continuous blood flow measurements. The femoral vein was cannulated to allow injection of the compounds. Animals were allowed 30 min to stabilize and were then injected with either 1 mg kg^{-1} of L-Arg-3,4 which had been dissolved as a 1 mg ml^{-1} stock solution in saline or an equivalent volume of saline. Following administration of the compound, rats were continuously monitored for 60 min, after which time anaesthesia was terminated and rats allowed to waken.

Transient forebrain ischaemia

All animal procedures were approved by the Home Office. Animals were anaesthetized as described above, and a thermistor inserted into the left temporal muscle for recording body temperature. A dorsal midline incision was made in the neck, and the vertebral arteries were identified and occluded at the level of C1 using a monopolar electrode. The incision was closed, animals allowed to recover from anaesthesia and returned to their cages for 24 h. After this time, animals were re-anaesthetized, and the common carotid arteries (CCAs) exposed. Ischaemia was induced by occluding the CCAs with microvascular clips for 15 min, after which the animals were allowed to recover, and were returned to their cages. Prior to ischaemia, animals were randomly allocated to either sham, saline control or L-Arg-3,4 groups. Sham animals had the CCAs exposed, but not occluded. Animals received either 1 mg kg^{-1} L-Arg-3,4 (prepared as above) or an equivalent volume of saline 15 min prior to ischaemia. The L-Arg-3,4 and saline were prepared immediately prior to the experiment, and the experimenter was blinded as to the identity of the substance to be injected.

Seventy-two hours after the termination of ischaemia, animals were terminally anaesthetized and transcardially perfused with 4% paraformaldehyde. The brains were processed for histology, and 20 μm sections stained with haematoxylin and eosin. Neuronal damage was assessed by counting the number of live and dead cells in a single 20 $\times$ field in CA1 and CA3 pyramidal cell layers by a blinded assessor.

Results

L-Arg-3,4 prevents ischaemic cell death

One hour of ischaemia generated reproducible neurodegeneration in the pyramidal cell layer in hippocampal slice cultures of approximately $38 \pm 2\%$ as determined by PI staining (Figure 2). Cell death in untreated control cultures from individual ischaemia experiments was not statistically different ($P = 0.70$), and, therefore, ischaemic controls were combined into a single group ($n = 149$). Incubation of cultures in 300 μM L-Arg-3,4 pre-, during, and post-ischaemia resulted in a significant reduction of neurodegeneration (Figure 4) to $23 \pm 4\%$ (39% protection, $P < 0.01$, $n = 34$).

L-Arg-3,4 prevents ischaemic cell death when administration is delayed

To determine the effective time window after injury, administration of L-Arg-3,4 was delayed until after the completion of the ischaemia and applied at 0, 10, 30, 60, and 120 min post-injury. As a comparison, parallel cultures were treated with 10 μM MK-801 at 0 and 30 min post ischaemia. Delayed application of 300 μM L-Arg-3,4 significantly decreased cell death as compared to controls at 0, 10, 30, and 60 min post-injury (Figure 4) reducing damage to $23 \pm 3\%$ (37% protection, $P < 0.01$, $n = 36$), $22 \pm 3\%$ (40% protection, $P < 0.01$, $n = 37$), $26 \pm 3\%$ (27% protection, $P < 0.05$, $n = 39$), and $26 \pm 3\%$ (27% protection, $P < 0.05$, $n = 31$), respectively. Although damage was reduced to $29 \pm 5\%$ at 120 min post injury, the 20% protection was not significant ($P > 0.05$, $n = 11$). In comparison, 10 μM MK-801 administered at 0 min after ischaemia (Figure 4) significantly reduced damage to $24 \pm 3\%$ (35% protection, $P < 0.05$, $n = 27$), however if administration was delayed by
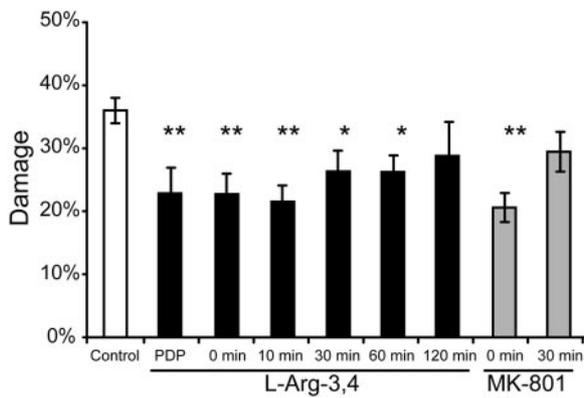
Figure 4 Damage after 1 h of ischaemia as determined by PI staining in the CA1 pyramidal cell layer was significantly reduced by 300 μM L-Arg-3,4 when administered either pre- during and post-injury (PDP) or when administered at indicated time points after ischaemia. Reduction of cell death was significant when L-Arg-3,4 administration was delayed for as long as 60 but not 120 min post ischaemia. As a comparison, 10 μM MK-801 lost its protective efficacy when administration was delayed by 30 min. Cell death was assessed 24 h post-injury in all groups. Data is presented as mean±s.e.mean with * indicating $P < 0.05$ and ** indicating $P < 0.01$ vs control.
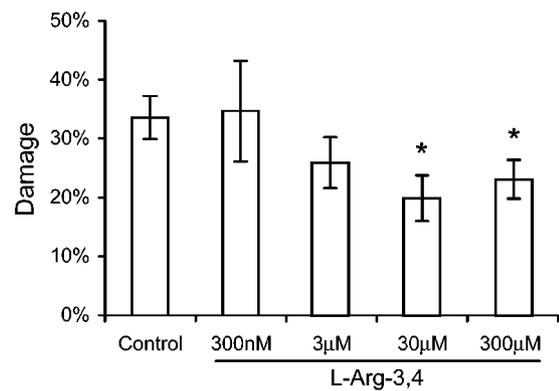

Figure 5 Dose response of reduction in damage in the CA1 pyramidal cell layer for different concentrations of L-Arg-3,4 administered immediately after ischaemia. Although 3 μM did not significantly reduce injury, both 30 and 300 μM significantly reduced damage in the CA1 cell layer. Data is presented as mean±s.e.mean with * indicating $P < 0.05$ vs control.
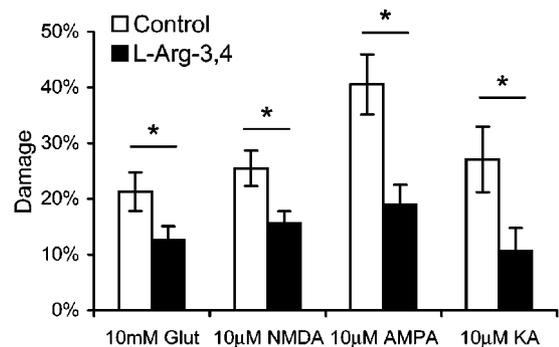

Figure 6 L-Arg-3,4 significantly reduced cell death in different models of excitotoxicity. Pre-, during, and post-injury administration of L-Arg-3,4 significantly prevented CA1 pyramidal cell death when cultures were incubated in either 10 mM glutamate, 10 μM NMDA, or 10 μM AMPA for 3 h. In addition, L-Arg-3,4 significantly prevented cell loss in the CA3 pyramidal cell layer after a 3 h incubation in 10 μM kainate. Cell death was assessed 24 h post-injury in all groups. Data is presented as mean±s.e.mean with * indicating $P < 0.05$ vs control.

30 min, MK-801 was no longer protective reducing damage to 29±3% (18% protection, $P > 0.05$, $n = 27$).

Effective dose response of L-Arg-3,4 against ischaemia

The effective post-injury dose for neuroprotection against ischaemia was tested with concentrations of L-Arg-3,4 ranging from 300 nM to 300 μM. A dose of 300 μM was initially chosen for all studies based on previous data in a model of hypoxic injury which indicated that 300 μM was an optimal dose (data not shown). Untreated controls from separate experiments were not significantly different ($P = 0.9$) with an aggregate damage of 34±9% and were combined into a single group ($n = 47$). At 300 nM, L-Arg-3,4 did not reduce damage (Figure 5), however, at 3, 30, and 300 μM, the compound did reduce damage to 19±5% (43% protection, $P < 0.06$, $n = 14$), 11±3% (67% protection, $P < 0.05$, $n = 8$), and 23±3% (32% protection, $P < 0.05$, $n = 36$), respectively as compared to the untreated group. Groups treated with 3, 30, or 300 μM L-Arg-3,4 were not significantly different from each other.

L-Arg-3,4 prevents excitotoxic cell death

Administration of 300 μM L-Arg-3,4 significantly reduced cell death in the CA1 pyramidal cell layer generated by 10 mM Glut (Figure 6) from 21±3% damage in controls ($n = 23$) to 13±3% in treated cultures (41% protection, $P < 0.05$, $n = 23$) suggesting that it could be a glutamate receptor antagonist. To determine if its actions were glutamate receptor subtype specific, L-Arg-3,4 was tested against 10 μM NMDA, 10 μM AMPA, and 10 μM kainate in separate experiments which produced regionally specific cell death as shown in Figure 2. Administration of 300 μM L-Arg-3,4 significantly reduced the cell death in the CA1 pyramidal layer generated by 10 μM NMDA (Figures 2 and 6) from 25±3% damage in controls

($n = 42$) to 16±2% in treated cultures (38% protection, $P < 0.05$, $n = 43$) or 10 μM AMPA (Figure 6) from 41±5% damage in controls ($n = 21$) to 19±4% in treated cultures (53% protection, $P < 0.01$, $n = 22$). Furthermore, 300 μM L-Arg-3,4 significantly reduced the cell death in the CA3 pyramidal layer due to 10 μM kainate (Figures 2 and 6) from 27±6% damage in controls ($n = 21$) to 11±4% in treated cultures (61% protection, $P < 0.05$, $n = 24$).

L-Arg-3,4 does not suppress synaptic transmission

Bath application of 300 μM L-Arg-3,4 did not grossly affect evoked responses from acute hippocampal slices. Individual evoked responses from a single slice before, during, and after L-Arg-3,4 application showed that the compound had no effect on evoked responses (Figure 7A). This lack of effect was in contrast to the effect of 10 μM DNQX which blocked the evoked response completely (Figure 7B). The population spike of a single slice to a sub-maximal stimulus was not

affected by L-Arg-3,4 infusion nor its wash out. However, in the same slice, 10 μM DNQX eliminated all transmission within 5 min (Figure 7B). S/R curves for a slice before, during, and after L-Arg-3,4 were not affected by bath
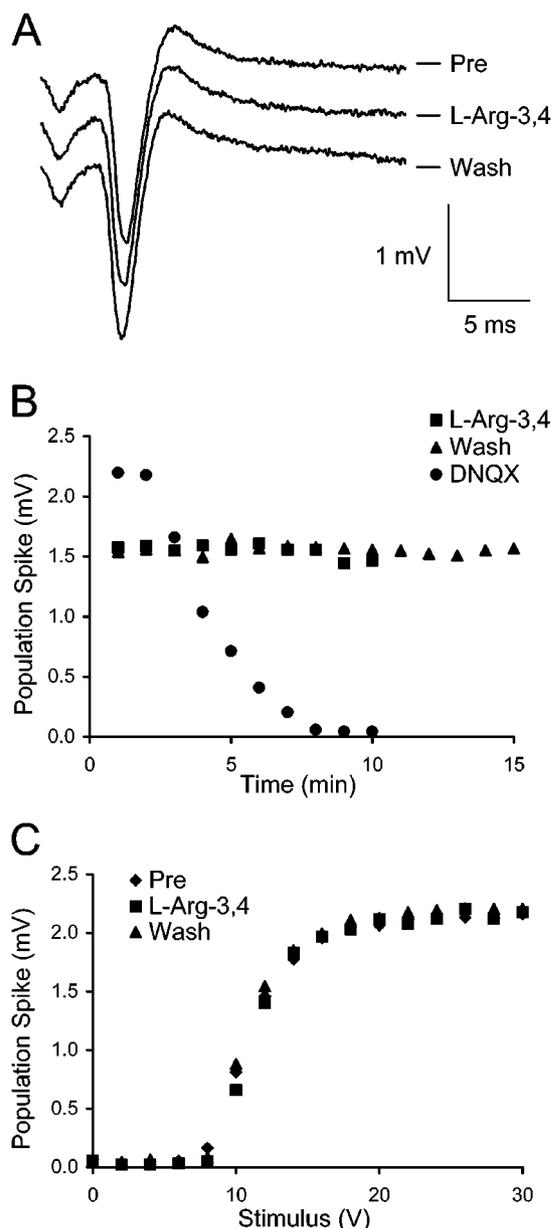

Figure 7 L-Arg-3,4 did not affect synaptic transmission as measured by field potential recordings of evoked responses in acute hippocampal slices. (A) Evoked potentials at the same stimulus voltage from an acute hippocampal slice under three different conditions. Bath application of L-Arg-3,4 did not affect the shape of the evoked responses. (B) The magnitude of the population spike in response to the same stimulus voltage plotted over time under different conditions. Incubation in 300 μM L-Arg-3,4 did not affect the evoked response over the 10 min infusion, nor did a subsequent wash for 15 min. However, bath application of 10 μM DNQX quickly inhibited synaptic transmission which was completely blocked within 10 min. (C) Stimulus-response curves from the same acute slice were not affected by the three incubation conditions. Conditions were as follows: Pre, before application of drug; L-Arg-3,4, 10 min bath application of 300 μM L-Arg-3,4; Wash, 15 min of wash; DNQX, bath application of 10 μM DNQX.

application of 300 μM L-Arg-3,4 (Figure 7C). All S/R curves were fitted to a sigmoidal function (Equation 1) so that comparisons between aggregate S/R curves could be made (Table 1). None of the parameters was significantly affected by L-Arg-3,4 infusion as determined by a one way ANOVA for each parameter.

L-Arg-3,4 prevents free-radical mediated cell death

Administration of 300 μM L-Arg-3,4 significantly reduced cell death in the CA1 pyramidal cell layer caused by a 3 h incubation in 100 μM duroquinone (Figures 2 and 8) suggesting that it may be quenching free-radicals. Injury was reduced from $40 \pm 5\%$ in untreated controls ($n = 21$) to $21 \pm 5\%$ in treated cultures (46% protection, $P < 0.05$, $n = 21$).

L-Arg-3,4 decreases AMPA or NMDA stimulated superoxide production

Production of superoxide was reliably measured fluorescently with HEt as previously reported (Bindokas *et al.*, 1996;

Table 1 Fitting parameters for stimulus-response curves

	R_{max} (mV)	V_{50} (V)	m	n
Pre	2.61 ± 1.16	19.28 ± 6.02	0.32 ± 0.18	6
L-Arg-3,4	2.71 ± 1.31	15.98 ± 5.12	0.59 ± 0.48	6
Wash	2.38 ± 0.83	15.07 ± 5.39	0.78 ± 0.60	3
P	0.92	0.48	0.29	

Parameters which best fit the stimulus-response curves to sigmoidal curves under the three experimental conditions are presented. The electrophysiological response of acute hippocampal slices was measured in the CA1 region from stimuli applied to the Schaffer collaterals in the CA3 region. the response of the tissue to increasing stimuli demonstrated a typical non-linear response which was fitted to the sigmoidal function of Equation 1. The best fit parameters were calculated and are presented as mean $\pm$ s.d. Also shown are the numbers (n) in each experimental group as well as the significance level (P) calculated from a one way ANOVA. No parameters were significantly affected by L-Arg-3,4. Conditions were as follows: Pre, before application of drug; L-Arg-3,4, after a 10 min bath application of 300 μM L-Arg-3,4; Wash, after 15 min of wash.
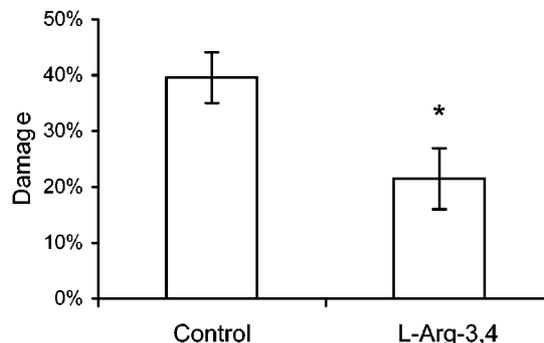

Figure 8 L-Arg-3,4 significantly reduced CA1 pyramidal cell death due to superoxide generation. A 3 h incubation in 100 μM duroquinone caused delayed neuronal cell death as measured 24 h post-injury which was significantly attenuated by treatment with 300 μM L-Arg-3,4 pre-, during, and post-injury. Data is presented as mean $\pm$ s.e.mean with * indicating $P < 0.05$ vs control.

Carriedo et al., 1998). In the AMPA stimulation experiments, baseline superoxide production was measured to be 2.06 ± 1.60 AU min^{-1} ($n = 16$) and was not affected by 300 μM L-Arg-3,4, 2.55 ± 2.02 AU min^{-1} ($P > 0.6$, data not shown). Stimulation of glutamate receptors by 10 μM AMPA significantly increased the rate of superoxide production approximately 5 fold to 10.65 ± 3.70 AU min^{-1} ($n = 18$, $P < 0.001$, Figure 9A). The subsequent addition of 300 μM L-Arg-3,4, in the continued presence of 10 μM AMPA, significantly reduced the rate of superoxide production by approximately half to 5.07 ± 1.94 AU min^{-1} compared to the rate with AMPA alone ($n = 4$, $P < 0.01$), although this rate was still significantly elevated from baseline ($P < 0.01$).

In response to stimulation by 500 μM NMDA, superoxide production was increased approximately 50% above baseline
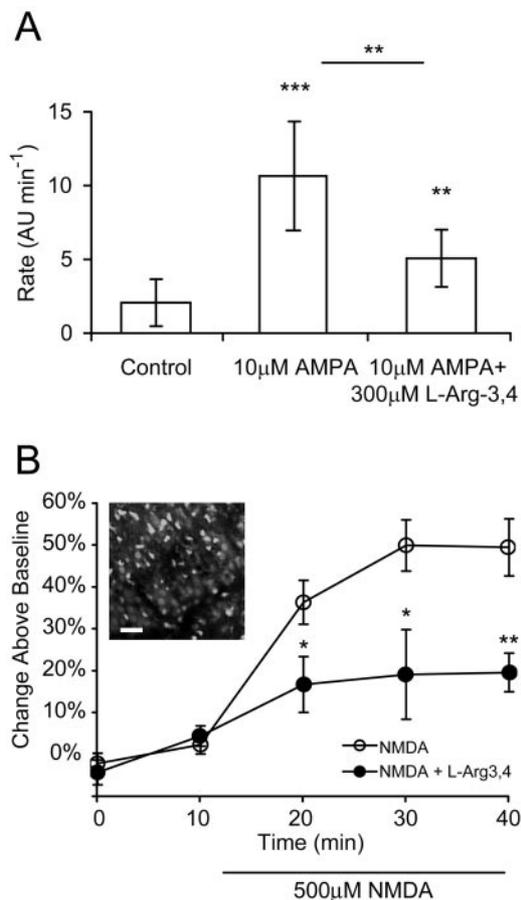

Figure 9 Induction of superoxide production was inhibited by L-Arg-3,4. (A) The rate of superoxide production was increased in the CA1 pyramidal cell layer of cultures exposed to 10 μM AMPA as measured by HEt fluorescence as compared to the pre-exposure baseline rate. Subsequent addition of 300 μM L-Arg-3,4 in the continued presence of 10 μM AMPA, significantly reduced the rate as compared with AMPA alone. However, this rate was still greater than the baseline rate. Data is presented as mean $\pm$ s.d. with ** indicating $P < 0.01$, and *** indicating $P < 0.001$. (B) An increases of superoxide production in single CA1 pyramidal cells in response to 500 μM NMDA stimulation was visualized with confocal microscopy (inset, scale bar = 50 μm) and quantified. NMDA stimulation increased superoxide production 50% above basal levels, and this increase was reduced to approximately 20% with pre-treatment by 300 μM L-Arg-3,4. Data is presented as mean $\pm$ s.e.mean with * indicating $P < 0.05$, and ** indicating $P < 0.01$ vs NMDA alone.

(Figure 9B, $n = 7$ cultures, 42 cells). In agreement with the AMPA data, this increase in superoxide production was diminished in the presence of 300 μM L-Arg-3,4 ($n = 5$ cultures, 30 cells) by approximately half and was significantly reduced at 10 ($36 \pm 5\%$ vs $16 \pm 7\%$, $P < 0.05$), 20 ($49 \pm 6\%$ vs $19 \pm 11\%$, $P < 0.05$), and 30 min ($49 \pm 7\%$ vs $19 \pm 5\%$, $P < 0.01$) after the start of stimulation.

L-Arg-3,4 decreases NO production but does not inhibit NOS

Production of NO was reliably measured by the conversion of DAF-2 to its fluorescent product triazolofluorescein both within organotypic cultures and in the cell-free microplate assay. In cultures subjected to ischaemia for 60 min, NO production, determined by an increase in fluorescence of the CA1 pyramidal cell layer, increased $13 \pm 3\%$ above pre-ischaemia levels ($n = 59$) whereas pre-incubation in 300 μM L-Arg-3,4 significantly reduced this increase to $1 \pm 1\%$ (Figure 10A, $n = 56$, $P < 0.001$). In separate experiments, 500 μM NMDA also significantly elevated NO production in CA1 $156 \pm 45\%$ after 30 min compared to pre-stimulation levels (Figure 10B, $n = 14$, $P < 0.01$). Pre-incubation in 300 μM L-Arg-3,4 prevented an increase in NO production compared to baseline levels ($24 \pm 40\%$, $n = 5$) although this level was not significantly decreased compared to NMDA stimulated NO production in the absence of L-Arg-3,4.

The direct effect of L-Arg-3,4 on NOS was determined in a cell free assay. Control samples generated NO at a rate of 31 ± 3 AU min^{-1} ($n = 8$) whereas samples without tissue extract or DAF-2 did not change fluorescence over time (data not shown) indicating that the change in fluorescence was due to conversion of DAF-2. The conversion of DAF-2 to its fluorescent product was specifically mediated by NO as increasing concentrations of L-NAME, an inhibitor of NOS, significantly decreased the rate by 57% at 10 mM (Figure 10C, $n = 8$ per group, all concentrations of L-NAME $P < 0.01$). In contrast, increasing concentrations of L-Arg-3,4 up to 300 μM inhibited the production of NO by a maximum of 11%, which was not significant. Furthermore, this non-significant inhibition was not dose dependent (Figure 10C, $n = 8$ per group).

L-Arg-3,4 prevents ischaemic cell death in vivo

Intravenous administration of 1 mg kg^{-1} L-Arg-3,4 did not affect blood pressure, heart rate or respiration in anaesthetized rats, and no motor deficits or aberrant behaviour was noted in animals recovering from anaesthesia. Transient forebrain ischaemia was induced in rats using the rat four vessel occlusion model. In control animals, significant neuronal loss was observed in the hippocampus of animals 72 h after a 15 min ischaemic episode. This neuronal loss was primarily in the CA1 region where only 29.7 ± 10.6 pyramidal cells per 20 $\times$ field were observed in a total of 14 hippocampi from seven animals. This was in comparison to 92.3 ± 3.4 in sham operated animals. A smaller degree of neuronal loss was also observed in the CA3 region, where the number of neurones was reduced from 94.2 ± 8.3 to 49 ± 10.1 ($n = 14$). In animals pre-treated with 1 mg kg^{-1} L-Arg-3,4 15 min prior to induction of ischaemia, neuronal loss in CA1 was significantly reduced, with 72.0 ± 7.2 ($n = 10$) neurones visible in

each field ($P < 0.01$ vs untreated animals). Neuronal loss in CA3 was reduced (to 61.5 ± 8.0 cells per $20 \times$ field), but not
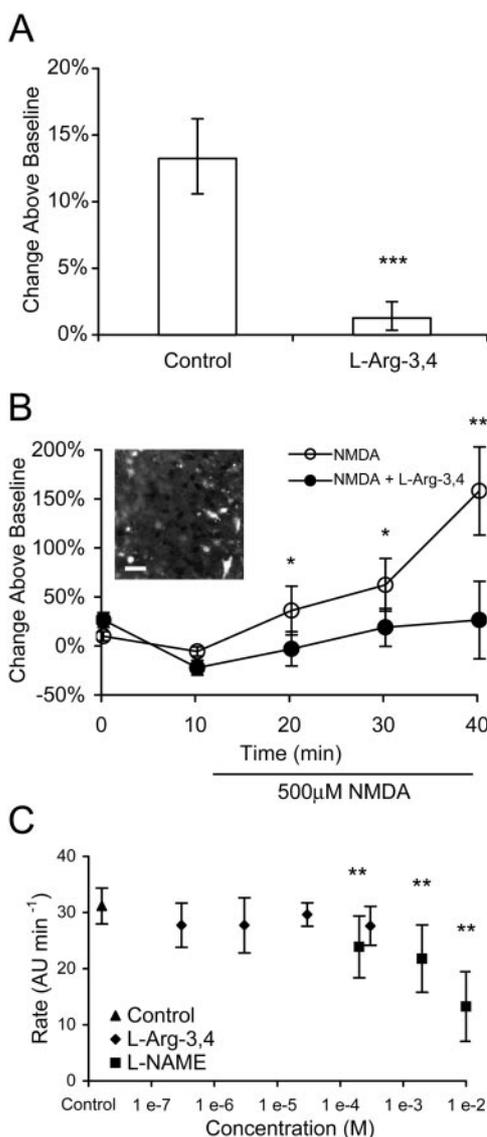

Figure 10 The effect of L-Arg-3,4 on NO production in different paradigms is presented. (A) The production of NO in the CA1 pyramidal cell layer due to 60 min of ischaemia was significantly inhibited by L-Arg-3,4 as measured by the conversion of DAF-2 to its fluorescent product. Data is presented as mean±s.e.mean. (B) Increased production of NO was visualized with confocal microscopy (inset, scale bar = 50 μm). Stimulation of cultures with 500 μM NMDA significantly increased NO production in the CA1 pyramidal cell layer as compared to baseline levels. Pre-incubation of cultures in 300 μM L-Arg-3,4 prevented this increase such that NO production was not significantly different from baseline, although this level was not significantly decreased from NMDA stimulated levels. (C) The rate of NO production by crude cortical homogenate in a cell free assay was not affected by L-Arg-3,4 and was expressed as the increase in fluorescence intensity in arbitrary units per min. Increasing concentrations of L-Arg-3,4 from 300 nM to 300 μM did not significantly affect the rate of NO production. This negative result was in contrast to the effects of L-NAME which did significantly inhibit NO production in a dose dependent manner at concentrations ranging from 200 μM to 10 mM indicating that L-Arg-3,4 did not directly inhibit NOS. Data is presented as mean±s.d. with * indicating $P < 0.05$, ** indicating $P < 0.01$, and *** indicating $P < 0.001$.

to a significant degree. These results are summarized in Figure 11.

Discussion

Organotypic hippocampal slice culture models are ideal preparations for the search of novel drugs because they allow for the rapid screening of a large number of compounds. In contrast to conventional high throughput screens, *a priori* knowledge of a proposed mechanisms of action is not necessary for the discovery of a novel drug with these systems. These culture preparations possess the added advantage over other *in vitro* systems of maintaining several key similarities to *in vivo* models including delayed neurodegeneration and selective vulnerability of either the CA1 or CA3 pyramidal cell layer depending on the injury paradigm and severity. Utilizing these models of neurodegeneration, we have begun to elucidate the mechanism of action of L-Arg-3,4 which could be a potentially therapeutic compound for the treatment of a myriad of CNS degenerative conditions, particularly because it does not affect synaptic transmission.

We have extended previous results obtained with a model of hypoxia to a more severe *in vitro* injury paradigm of ischaemia (oxygen and glucose deprivation) and have shown that L-Arg-3,4 significantly prevented CA1 cell loss after 1 h of ischaemia (Figure 4). A critical parameter for a clinically useful, experimental, therapeutic compound is how long after the insult it can be administered and still remain effective, i.e. its therapeutic window. To determine the available therapeutic window for L-Arg-3,4, administration was delayed for up to 120 min post-ischaemia and, surprisingly, it was still neuroprotective when administration was delayed for as long as 60 min. This therapeutic window is over twice as long as that for MK-801, D-APV, or dextromethorphan which lose effectiveness if administration is delayed for 30 min in models of excitotoxicity (Hartley & Choi, 1989) and ischaemia (Figure 4), suggesting that the mechanism of action of L-Arg-3,4 is unlikely to be at the level of the NMDA receptor.

Given the well established involvement of glutamate in the pathophysiological sequelae of ischaemia, we tested whether
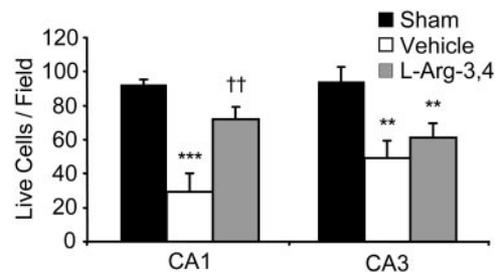

Figure 11 Effect of 1 mg kg^{-1} L-Arg3,4 administered 15 min prior to global forebrain ischaemia in rats. The number of live cells in a ×20 field was determined 3 days after reperfusion by a blinded observer. Neuronal damage occurred primarily in the CA1 pyramidal cell layer with damage also present in the CA3 pyramidal cell layer compared to sham operated controls. Pre-treatment with L-Arg3,4 was significantly neuroprotective in CA1, but not in CA3. Data presented as mean±s.d. with ** indicating $P < 0.01$, *** indicating $P < 0.001$ vs the same region in sham controls, †† indicating $P < 0.01$ vs CA1 in ischaemic group; $n = 7$–9 animals in each group.

L-Arg-3,4 was neuroprotective against EAA mediated cell death. L-Arg-3,4 significantly prevented cell death due to glutamate, NMDA, AMPA, and kainate toxicity (Figure 6). These results are similar to those of Weiss *et al.* (1990) who demonstrated that high doses of nifedipine (100 μM) could prevent cell loss in cortical cell cultures due to AMPA, kainate, or quinolinate exposure, and that this effect was not due to a direct inhibition of agonist mediated cell currents. However, nifedipine was not able to prevent toxicity due to NMDA or glutamate (Weiss *et al.*, 1990; Hartley & Choi, 1989). Neither 100 μM nifedipine nor diltiazem could prevent the loss of electrical activity in acute hippocampal slices caused by NMDA (Longo *et al.*, 1994), suggesting that the dihydrophyridines can prevent excitotoxic cell death, probably by limiting cellular Ca^{2+} loading, provided that loading is minimal (Weiss *et al.*, 1990; Hartley & Choi, 1989). Nifedipine is not neuroprotective in an organotypic hippocampal model of hypoxia in which cellular Ca^{2+} loading is likely to be less severe than during ischaemia (Pringle *et al.*, 1996). Therefore, the actions of L-Arg-3,4 appear to be more robust than L-type VSCC antagonists as it was neuroprotective in more severe injury paradigms such as NMDA mediated excitotoxicity as well as ischaemia.

Given its structural similarity to spermidine, L-Arg-3,4 could be acting at the polyamine site of the NMDA receptor. At low concentrations, spermine and spermidine can exacerbate NMDA toxicity both *in vivo* (Gimenez-Llort *et al.*, 1996) and *in vitro* (Sparapani *et al.*, 1997), but at higher concentrations ($\geqslant$ 1 mM), these polyamines can be protective (Ferchmin *et al.*, 2000). L-Arg-3,4 does not potentiate NMDA receptor activation because it did not exacerbate NMDA mediated neurotoxicity in our studies (Figure 6), and therefore, probably does not interact with the polyamine site on the NMDA receptor. Given its structural similarity to sFTX, L-Arg-3,4 could be antagonizing VSCC thereby preventing Ca^{2+} loading in vulnerable neurons. Alternatively, L-Arg-3,4 could be acting non-specifically at a variety of cation permeable channels in a similar manner to other polyamines such as spermine and arcaine which block the open channel (Scott *et al.*, 1993). Cherksey *et al.* (1991) investigated the ability of a series of structurally related compounds to block VSCC in Purkinje cells and at the squid giant synapse. Of the series of compounds they tested, one was identical to L-Arg-3,4, and they found that it did not inhibit Ca^{2+} currents, indicating that our compound probably does not inhibit VSCC. It is also unlikely that L-Arg-3,4 inhibits either N or P/Q-type VSCC responsible for neurotransmitter release in the hippocampus as inhibitors of these channels decrease evoked population spikes by approximately 50% (Takahashi & Momiyama, 1993). In our experiments, L-Arg-3,4 did not affect synaptic transmission in any way as determined by measuring evoked field responses in acute hippocampal slices (Figure 7 and Table 1) reaffirming that it does not interact with VSCC. This lack of effect was in sharp contrast to the effect of 10 μM DNQX which abolished all synaptic transmission within 10 min of exposure indicating that L-Arg-3,4 does not alter transmission mediated by non-NMDA receptors.

Its lack of electrophysiological effects in combination with its ability to prevent ischaemic and excitotoxic cell death by both NMDA and non-NMDA receptor agonists suggests that L-Arg-3,4 may be acting down stream of receptor and or

channel activation. Its very long therapeutic window also suggests that it may target a nexus of the pathological sequelae which is common to these models of cell death especially since NMDA antagonists, such as MK-801, have a much shorter therapeutic window of less than 30 min in models of excitotoxicity (Hartley & Choi, 1989) or ischaemia in our hands (Figure 4). Zhang & Lipton (1999) have shown that ischaemia in acute hippocampal slices causes an initial rise in intracellular Ca^{2+} which is mediated by NMDA receptors because it can be blocked by MK-801. A second rise of intracellular Ca^{2+} mediated by release from mitochondria can be blocked by mitochondria-specific Ca^{2+} exchanger inhibitors (Zhang & Lipton, 1999). Under conditions of oxidative stress, excitotoxicity, or Ca^{2+} overload, mitochondria become a significant source of free-radicals which can overload endogenous scavenging systems, damage cellular components, and lead to cell death (Bindokas *et al.*, 1996; Carriedo *et al.*, 1998).

To test the hypothesis that the protection afforded by L-Arg-3,4 was due to its ability to affect ROS mediated cell death, cultures were injured by incubation in 100 μM DQ which specifically generates superoxide by disruption of the mitochondria electron transport chain (Wilde *et al.*, 1997). L-Arg-3,4 significantly protected against free-radical mediated injury suggesting that it may quench ROS (Figure 8). The effect of the compound on superoxide production was directly measured with the non-invasive, fluorescent reporter HEt in response to AMPA as well as NMDA stimulation of glutamate receptors (Figure 9). As reported previously, AMPA or NDMA stimulation resulted in a robust and sustained increase in the rate of superoxide production (Rozov & Burnashev, 1999; Carriedo *et al.*, 1998) which was significantly reduced by L-Arg-3,4 in the continued presence of the excitotoxin. These results clearly demonstrate that one of the protective mechanisms of action of L-Arg-3,4 is to reduce the rate of superoxide production in response to injurious stimuli which could be the basis of its neuroprotective actions in the diverse injury paradigms used in these experiments. Polyamines, such as spermine and spermidine, are known to directly scavenge ROS *via* a charge transfer process which can protect DNA from ROS mediated degradation (Ha *et al.*, 1998). The spermidine moiety of L-Arg-3,4 could be functioning in the same manner as free spermidine. In addition, the L-Arg-3,4 contains two primary and one secondary amine which potentially could also act as scavengers by the same charge transfer process hypothesized for spermidine. Other possibilities exist which could be examined in subsequent studies such as an effect of L-Arg-3,4 directly on mitochondria to limit ROS production in a more direct manner.

In addition to superoxide, other ROS are generated during ischaemia and EAA mediated cell death. Nitric oxide is a highly reactive free-radical which has several physiological functions. It has been implicated in the pathological sequelae in ischaemic and excitotoxic cell death and can cause a perturbation of iron metabolism, inhibition of mitochondria electron transport, DNA damage, and ADP-ribosylation (Dawson *et al.*, 1991; Cooper, 1999; Brown, 1999). Inhibitors of NOS decrease neuronal death in models of both excitotoxicity and ischaemia (Dawson *et al.*, 1991; Maiese *et al.*, 1993), and other polyamines with structural similarities to L-Arg-3,4 such as spermine, spermidine, putrescine,

arcaine, and agmatine are know inhibitors of NOS (Hu et al., 1994; Kabuto et al., 1995; Galea et al., 1996). L-Arg-3,4 significantly reduced NO production induced by ischaemia (Figure 10A), and also reduced an increase caused by toxic concentrations of NMDA (Figure 10B), although this reduction was not significant.

We further tested whether L-Arg-3,4 could inhibit the production of NO by NOS in a cell-free system, and found that it reduced NO production by approximately 10%, although this effect was not significant, nor was it dose dependent (Figure 10C). This effect was in contrast to the effects of L-NAME which significantly inhibited NOS and reduced NO production in a dose dependent manner. The results of this assay could be explained one of two ways. Either L-Arg-3,4 was slightly inhibiting the NOS directly and therefore preventing NO formation, or it was scavenging NO before it could react with the reporter, DAF-2. Although the assay could not discriminate between these two mechanisms, the net effect of L-Arg-3,4 on NOS was not significant.

The results of the cell free assay demonstrating that L-Arg-3,4 does not inhibit production of NO and the ischaemia model demonstrating a reduction of NO synthesis may appear contradictory, but are, in fact, consistent. Although L-Arg-3,4 does not have a direct effect on NOS, it may be inhibiting any one of the upstream steps in the ischaemic cascade which leads to increased NO production. A possible target for L-Arg-3,4 protective effects is the mitochondrion which has been implicated in contributing to cell death in response to the injury paradigms used in our study (Dugan et al., 1995; Rego et al., 2001; Lacza et al., 2001). Mitochondria are equipped with a specific mitochondrial NOS (mtNOS) which may regulate activity of the electron transport chain (Cleeter et al., 1994) as well as trigger release of sequestered Ca^{2+} and cytochrome c (Ghafourifar et al., 1999). It has been proposed that Ca^{2+} sequestration leads to activation of mtNOS and a local production of NO (Cleeter et al., 1994). This NO inhibits the electron transport chain, resulting in the formation of superoxide and other ROS which react with NO to form peroxynitrite. The peroxynitrite then triggers the release of Ca^{2+} as well as cytochrome c. It is the initial sequestration of Ca^{2+} by the mitochondria and not necessarily cytoplasmic Ca^{2+} loading which is responsible for initiation of cell death via disruption of the electron transport chain and production of NO (Budd & Nicholls, 1996; Wang & Thayer, 1996; Luetjens et al., 2000). It is tantalizing to speculate that L-Arg-3,4 may be inhibiting the mitochondrial Ca^{2+} uniporter in a manner similar to RU360 thereby preventing sequestration of Ca^{2+} (Unitt et al., 1999; Zazueta et al., 1999). By breaking the chain of pathological changes, the down stream mediators of cell damage and death, such as NO production, are inhibited. Taken together, our results indicate that the neuroprotection afforded by L-Arg-3,4 is not due to NO scavenging or NOS inhibition, but more likely due to inhibition of other pathological mechanisms, such as superoxide production or mitochondria Ca^{2+} loading, which in turn stimulate NO production.

Many compounds that block VSCC do not make good drug candidates because of their side-effect profile which includes significant depression of cardiovascular function (Bowersox et al., 1992). Therefore, although compounds such as the selective N-type channel blocker ω-conotoxin-MVIIA and the non-selective blocker ω-conotoxin-MVIIC are potently active in the organotypic hippocampal slice culture (OHSC) model of hypoxia-mediated neurodegeneration (Pringle et al., 1996), they are associated with profound hypotensive side-effects in vivo (Buchan et al., 1994). FTX is also lethal to mice when injected intra-peritoneally (Llinas et al., 1989) and, at a non-toxic dose, is associated with profound sedation. Intra-venous (i.v.) injection of 1 mg kg^{-1} L-Arg-3,4 produced no change in blood pressure clearly implying that the compound has little or no action at central calcium channels as predicted. In addition, no gross motor effects were observed when animals recovered from anaesthesia. Having determined that the compound was safe at 1 mg kg^{-1} i.v., we next investigated whether this dose was neuroprotective in an in vivo model of cerebral ischaemia. The 4-vessel occlusion model of transient forebrain ischaemia was chosen since this is the paradigm most closely modelled by the OHSC ischaemia model. L-Arg-3,4 was neuroprotective when administered i.v. 15 min prior to ischaemia mimicking the efficacy observed in vitro. This observation is important for two reasons. Firstly, it confirms that the compound is capable of acting centrally despite having no overt side-effects. Secondly, it confirms that neuroprotective efficacy observed in the OHSC ischaemia model can be translated into in vivo efficacy in a model of global forebrain ischaemia.

In summary, we have begun to study the neuroprotective mechanism of action of a novel compound, L-Arg-3,4, which prevents cell death in both in vitro and in vivo models of ischaemia. Surprisingly, delayed administration of L-Arg-3,4 after in vitro ischaemia (up to 60 min) was also neuroprotective. This extremely long therapeutic window in vitro is in contrast to that of NMDA antagonists, such as MK-801, which loses efficacy as early as 15 min post-injury (Hartley & Choi, 1989) or, in the present study, when delayed by 30 min after in vitro ischaemia. L-Arg-3,4 prevented cell death due to glutamate toxicity but was not receptor sub-type specific as it also prevented cell death due to NMDA, AMPA, and kainate in vitro. The compound did not inhibit synaptic transmission in vitro or cause any gross neurological effects in vivo, and therefore, was not likely to directly antagonize glutamate receptors or VSCC unlike a structurally similar compound, sFTX-3.3. L-Arg-3,4 also prevented superoxide mediated cell death and reduced the rate of superoxide production after AMPA or NMDA stimulation in vitro. The compound also decreased the production of NO due to ischaemia or NMDA stimulation, but did so without directly inhibiting NOS. Because it did not affect synaptic transmission, L-Arg-3,4 may engender fewer detrimental side effects than previous, experimental, therapeutic compounds. Given its robust neuroprotection in vitro and in vivo, future research in vivo is an appropriate next step as L-Arg-3,4 could be of potential benefit in the treatment of stroke and other neurodegenerative conditions such as traumatic brain injury, Alzheimer's disease, Parkinson's disease, and multiple sclerosis.

References

BINDOKAS, V.P., JORDAN, J., LEE, C.C. & MILLER, R.J. (1996). Superoxide production in rat hippocampal neurons: selective imaging with hydroethidine. *J. Neurosci.*, **16**, 1324–1336.

BOWERSOX, S.S., SINGH, T., NADASDI, L., ZUKOWSKA-GROJEC, Z., VALENTINO, K. & HOFFMAN, B.B. (1992). Cardiovascular effects of ω-conopeptides in conscious rats: mechanisms of action. *J. Cardiovasc. Pharmacol.*, **20**, 756–764.

BROWN, G.C. (1999). Nitric oxide and mitochondrial respiration. *Biochim. Biophys. Acta*, **1411**, 351–369.

BROWN, L.A., KEY, B.J. & LOVICK, T.A. (1999). Bio-imaging of nitric oxide-producing neurones in slices of rat brain using 4,5-diaminofluorescein. *J. Neurosci. Methods*, **92**, 101–110.

BUCHAN, A.M., GERTLER, S.Z., LI, H., XUE, D., HUANG, Z.G., CHAUNDY, K.E., BARNES, K. & LESIUK, H.J. (1994). A selective N-type Ca²⁺-channel blocker prevents CA1 injury 24 h following severe forebrain ischaemia and reduces infarction following focal ischaemia. *J. Cereb. Blood Flow Metab.*, **14**, 903–910.

BUDD, S.L. & NICHOLLS, D.G. (1996). Mitochondria, calcium regulation, and acute glutamate excitotoxicity in cultured cerebellar granule cells. *J. Neurochem.*, **67**, 2282–2291.

CARRIEDO, S.G., YIN, H.Z., SENSI, S.L. & WEISS, J.H. (1998). Rapid Ca²⁺ entry through Ca²⁺-permeable AMPA/Kainate channels triggers marked intracellular Ca²⁺ rises and consequent oxygen radical production. *J. Neurosci.*, **18**, 7727–7738.

CHERKSEY, B.D., SUGIMORI, M. & LLINAS, R.R. (1991). Properties of calcium channels isolated with spider toxin, FTX. *Ann. N. Y. Acad. Sci.*, **635**, 80–89.

CLEETER, M.W., COOPER, J.M., DARLEY-USMAR, V.M., MONCADA, S. & SCHAPIRA, A.H. (1994). Reversible inhibition of cytochrome c oxidase, the terminal enzyme of the mitochondrial respiratory chain, by nitric oxide. Implications for neurodegenerative diseases. *FEBS Lett*, **345**, 50–54.

COOPER, C.E. (1999). Nitric oxide and iron proteins. *Biochim. Biophys. Acta*, **1411**, 290–309.

DAWSON, V.L., DAWSON, T.M., LONDON, E.D., BREDT, D.S. & SNYDER, S.H. (1991). Nitric oxide mediates glutamate neurotoxicity in primary cortical cultures. *Proc. Natl. Acad. Sci. (U.S.A.)*, **88**, 6368–6371.

DUGAN, L.L., SENSI, S.L., CANZONIERO, L.M., HANDRAN, S.D., ROTHMAN, S.M., LIN, T.S., GOLDBERG, M.P. & CHOI, D.W. (1995). Mitochondrial production of reactive oxygen species in cortical neurons following exposure to N-methyl-D-aspartate. *J. Neurosci.*, **15**, 6377–6388.

DUPERE, J.R., MOYA, E., BLAGBROUGH, I.S. & USOWICZ, M.M. (1996). Differential inhibition of Ca²⁺ channels in mature rat cerebellar Purkinje cells by sFTX-3.3 and FTX-3.3. *Neuropharmacology*, **35**, 1–11.

FERCHMIN, P.A., PEREZ, D. & BIELLO, M. (2000). Spermine is neuroprotective against anoxia and N-methyl-D-aspartate in hippocampal slices. *Brain Res.*, **859**, 273–279.

FISHER, M. & SCHAEBITZ, W. (2000). An overview of acute stroke therapy: past, present, and future. *Arch. Intern. Med.*, **160**, 3196–3206.

GALEA, E., REGUNATHAN, S., ELIOPOULOS, V., FEINSTEIN, D.L. & REIS, D.J. (1996). Inhibition of mammalian nitric oxide synthases by agmatine, an endogenous polyamine formed by decarboxylation of arginine. *Biochem. J.*, **316**, 247–249.

GHAFOURIFAR, P., SCHENK, U., KLEIN, S.D. & RICHTER, C. (1999). Mitochondrial nitric-oxide synthase stimulation causes cytochrome c release from isolated mitochondria. Evidence for intramitochondrial peroxynitrite formation. *J. Biol. Chem.*, **274**, 31185–31188.

GIMENEZ-LLORT, L., FERRE, S., DE VERA, N. & MARTINEZ, E. (1996). Motor depressant effects of systemically administered polyamines in mice: involvement of central NMDA receptors. *Eur. J. Pharmacol.*, **318**, 231–238.

HA, H.C., SIRISOMA, N.S., KUPPUSAMY, P., ZWEIER, J.L., WOSTER, P.M. & CASERO-RA, J. (1998). The natural polyamine spermine functions directly as a free radical scavenger. *Proc. Natl. Acad. Sci. (U.S.A.)*, **95**, 11140–11145.

HARTLEY, D.M. & CHOI, D.W. (1989). Delayed rescue of N-methyl-D-aspartate receptor-mediated neuronal injury in cortical culture. *J. Pharmacol. Exp. Ther.*, **250**, 752–758.

HU, J., MAHMOUD, M.I. & EL FAKAHANY, E.E. (1994). Polyamines inhibit nitric oxide synthase in rat cerebellum. *Neurosci. Lett.*, **175**, 41–45.

KABUTO, H., YOKOI, I., HABU, H., ASAHARA, H. & MORI, A. (1995). Inhibitory effect of arcaine on nitric oxide synthase in the rat brain. *Neuroreport*, **6**, 554–556.

KRISTIAN, T. & SIESJO, B.K. (1998). Calcium in ischemic cell death. *Stroke*, **29**, 705–718.

LACZA, Z., PUSKAR, M., FIGUEROA, J.P., ZHANG, J., RAJAPAKSE, N. & BUSIJA, D.W. (2001). Mitochondrial nitric oxide synthase is constitutively active and is functionally upregulated in hypoxia. *Free Radic. Biol. Med.*, **31**, 1609–1615.

LLINAS, R., SUGIMORI, M., LIN, J.W. & CHERKSEY, B. (1989). Blocking and isolation of a calcium channel from neurons in mammals and cephalopods utilizing a toxin fraction (FTX) from funnel-web spider poison. *Proc. Natl. Acad. Sci. (U.S.A.)*, **86**, 1689–1693.

LONGO, R., SAGRATELLA, S. & SCOTTI, D.C. (1994). Effects of calcium antagonists on hypoxic and NMDA injury in rat hippocampal slices. *Life Sci.*, **55**, 455–462.

LUETJENS, C.M., BUI, N.T., SENGPIEL, B., MUNSTERMANN, G., POPPE, M., KROHN, A.J., BAUERBACH, E., KRIEGLSTEIN, J. & PREHN, J.H. (2000). Delayed mitochondrial dysfunction in excitotoxic neuron death: cytochrome c release and a secondary increase in superoxide production. *J. Neurosci.*, **20**, 5715–5723.

MAIESE, K., BONIECE, I., DEMEO, D. & WAGNER, J.A. (1993). Peptide growth factors protect against ischemia in culture by preventing nitric oxide toxicity. *J. Neurosci.*, **13**, 3034–3040.

MURRAY, C.J. & LOPEZ, A.D. (1997). Mortality by cause for eight regions of the world: Global Burden of Disease Study. *Lancet*, **349**, 1269–1276.

PIANTADOSI, C.A. & ZHANG, J. (1996). Mitochondrial generation of reactive oxygen species after brain ischemia in the rat. *Stroke*, **27**, 327–331.

PRINGLE, A.K., BENHAM, C.D., SIM, L., KENNEDY, J., IANNOTTI, F. & SUNDSTROM, L.E. (1996). Selective N-type calcium channel antagonist ω conotoxin MVIIA is neuroprotective against hypoxic neurodegeneration in organotypic hippocampal-slice cultures. *Stroke*, **27**, 2124–2130.

PRINGLE, A.K., IANNOTTI, F., WILDE, G.J., CHAD, J.E., SEELEY, P.J. & SUNDSTROM, L.E. (1997). Neuroprotection by both NMDA and non-NMDA receptor antagonists in *in vitro* ischemia. *Brain Res.*, **755**, 36–46.

REGO, A.C., WARD, M.W. & NICHOLLS, D.G. (2001). Mitochondria control ampa/kainate receptor-induced cytoplasmic calcium deregulation in rat cerebellar granule cells. *J. Neurosci.*, **21**, 1893–1901.

ROZOV, A. & BURNASHEV, N. (1999). Polyamine-dependent facilitation of postsynaptic AMPA receptors counteracts paired-pulse depression. *Nature*, **401**, 594–598.

SCOTT, R.H., SUTTON, K.G. & DOLPHIN, A.C. (1993). Interactions of polyamines with neuronal ion channels. *TiNS*, **16**, 153–160.

SPARAPANI, M., DALL'OLIO, R., GANDOLFI, O., CIANI, E. & CONTESTABILE, A. (1997). Neurotoxicity of polyamines and pharmacological neuroprotection in cultures of rat cerebellar granule cells. *Exp. Neurol.*, **148**, 157–166.

TAKAHASHI, T. & MOMIYAMA, A. (1993). Different types of calcium channels mediate central synaptic transmission. *Nature*, **366**, 156–158.

UNITT, J.F., BODEN, K.L., WALLACE, A.V., INGALL, A.H., COOMBS, M.E. & INCE, F. (1999). Novel cobalt complex inhibitors of mitochondrial calcium uptake. *Bioorg. Med. Chem.*, **7**, 1891–1896.

WANG, G.J. & THAYER, S.A. (1996). Sequestration of glutamate-induced Ca2+ loads by mitochondria in cultured rat hippocampal neurons. *J. Neurophysiol.*, **76**, 1611–1621.

WARLOW, C.P. (1998). Epidemiology of stroke. *Lancet*, **352** (Suppl 3): SIII1–SIII4.

WEISS, J.H., HARTLEY, D.M., KOH, J. & CHOI, D.W. (1990). The calcium channel blocker nifedipine attenuates slow excitatory amino acid neurotoxicity. *Science*, **247**, 1474–1477.

WILDE, G.J., PRINGLE, A.K., WRIGHT, P. & IANNOTTI, F. (1997). Differential vulnerability of the CA1 and CA3 subfields of the hippocampus to superoxide and hydroxyl radicals *in vitro*. *J. Neurochem.*, **69**, 883–886.

YAMAUCHI, M., OMOTE, K. & NINOMIYA, T. (1998). Direct evidence for the role of nitric oxide on the glutamate-induced neuronal death in cultured cortical neurons. *Brain Res.*, **780**, 253–259.

ZAZUETA, C., SOSA-TORRES, M.E., CORREA, F. & GARZA-ORTIZ, A. (1999). Inhibitory properties of ruthenium amine complexes on mitochondrial calcium uptake. *J. Bioenerg. Biomembr.*, **31**, 551–557.

ZHANG, Y. & LIPTON, P. (1999). Cytosolic Ca^{2+} changes during *in vitro* ischemia in rat hippocampal slices: major roles for glutamate and Na^+-dependent Ca^{2+} release from mitochondria. *J. Neurosci.*, **19**, 3307–3315.